

# PROCEEDINGS OF SPIE

[SPIEDigitallibrary.org/conference-proceedings-of-spie](https://spiedigitallibrary.org/conference-proceedings-of-spie)

## A thesis to probe unique exoplanet regimes with micro-arcsecond astrometry and precision closure phases at CHARA and VLTI

Tyler Gardner, John Monnier, Francis Fekel, Jean-Baptiste Le Bouquin, Adam Scovera, et al.

Tyler Gardner, John D. Monnier, Francis C. Fekel, Jean-Baptiste Le Bouquin, Adam Scovera, Gail Schaefer, Stefan Kraus, Fred C. Adams, Narsireddy Anugu, Hayley Beltz, Jean-Philippe Berger, Theo ten Brummelaar, Claire L. Davies, Jacob Ennis, Douglas R. Gies, Keith J. C. Johnson, Pierre Kervella, Kaitlin M. Kratter, Aaron Labdon, Cyprien Lanthermann, Isaac Malsky, Emily Rauscher, Johannes Sahlmann, Benjamin R. Setterholm, "A thesis to probe unique exoplanet regimes with micro-arcsecond astrometry and precision closure phases at CHARA and VLTI," Proc. SPIE 12183, Optical and Infrared Interferometry and Imaging VIII, 121830Z (26 August 2022); doi: 10.1117/12.2630035

**SPIE.**

Event: SPIE Astronomical Telescopes + Instrumentation, 2022, Montréal, Québec, Canada

# A thesis to probe unique exoplanet regimes with micro-arcsecond astrometry and precision closure phases at CHARA and VLTI

Tyler Gardner<sup>a</sup>, John D. Monnier<sup>a</sup>, Francis C. Fekel<sup>b</sup>, Jean-Baptiste Le Bouquin<sup>c</sup>, Adam Scovera<sup>a</sup>, Gail Schaefer<sup>d</sup>, Stefan Kraus<sup>e</sup>, Fred C. Adams<sup>a,f</sup>, Narsireddy Anugu<sup>d</sup>, Hayley Beltz<sup>a</sup>, Jean-Philippe Berger<sup>c</sup>, Theo Ten Brummelaar<sup>d</sup>, Claire L. Davies<sup>e</sup>, Jacob Ennis<sup>a</sup>, Douglas R. Gies<sup>d</sup>, Keith J.C. Johnson<sup>g</sup>, Pierre Kervella<sup>h</sup>, Kaitlin M. Kratter<sup>i</sup>, Aaron Labdon<sup>j</sup>, Cyprien Lanthermann<sup>d</sup>, Isaac Malsky<sup>a</sup>, Emily Rauscher<sup>a</sup>, Johannes Sahlmann<sup>k</sup>, and Benjamin R. Setterholm<sup>a</sup>

<sup>a</sup>Astronomy Department, University of Michigan, Ann Arbor, MI 48109, USA

<sup>b</sup>Center of Excellence in Information Systems, Tennessee State University, Nashville, TN 37209, USA

<sup>c</sup>Univ. Grenoble Alpes, CNRS, IPAG, 38000 Grenoble, France

<sup>d</sup>The CHARA Array of Georgia State University, Mount Wilson Observatory, Mount Wilson, CA 91203, USA

<sup>e</sup>Astrophysics Group, Department of Physics & Astronomy, University of Exeter, Stocker Road, Exeter, EX4 4QL, UK

<sup>f</sup>Physics Department, University of Michigan, Ann Arbor, MI 48109, USA

<sup>g</sup>Department of Computer Sciences, University of Wisconsin, Madison, WI 53706, USA

<sup>h</sup>LESIA, Observatoire de Paris, Université PSL, CNRS, Sorbonne Université, Université Paris Cité, 5 place Jules Janssen, 92195 Meudon, France

<sup>i</sup>Department of Astronomy and Steward Observatory, Univ. of Arizona, 933 N Cherry Ave, Tucson, AZ, 85721, USA

<sup>j</sup>European Southern Observatory, Casilla 19001, Santiago 19, Chile

<sup>k</sup>RHEA Group for the European Space Agency (ESA), European Space Astronomy Centre (ESAC),, Camino Bajo del Castillo s/n, 28692 Villanueva de la Cañada, Madrid, Spain

## ABSTRACT

In this thesis work, we exploit the unique capabilities of long baseline interferometry to fill two gaps in exoplanet parameter space: 1) the discovery of new planets around stars more massive than the Sun (Project ARMADA), and 2) the characterization of known planets that are extremely close to their host star (Project PRIME). Current detection methods struggle to find exoplanets around hot (A/B-type) stars. We are pushing the astrometric limits of ground-based optical interferometers to carry out a survey of sub-arcsecond A/B-type binary systems with ARMADA. We are achieving astrometric precision at the few tens of micro-arcsecond level in short observations at CHARA/MIRC-X and VLTI/GRAVITY. This incredible precision allows us to probe the au-regime for giant planets orbiting individual stars of the binary system. We present the status of our survey, including our newly implemented etalon wavelength calibration method at CHARA, detection of new stellar mass companions, and non-detection limits down to a few Jupiter masses in some cases. With Project PRIME, we show that ground-based optical interferometry can be used to measure the orbit-dependent spectra of close-in “hot Jupiter”-type exoplanets with precision closure phases. Detecting the infrared spectra of such planets allows us to place useful constraints on atmosphere circulation models. We perform injection tests with MIRC-X and MYSTIC at

---

Further author information: (Send correspondence to T.G.)

T.G.: E-mail: [tgardne@umich.edu](mailto:tgardne@umich.edu)

CHARA for the hot Jupiter exoplanet *Ups And b* to show that we are reaching down to a contrast of 2e-4. The promise of both these methods demonstrate that optical interferometers are a valuable tool for probing unique regimes of exoplanet science.

**Keywords:** Interferometry, Astrometry, Exoplanets, Binary Systems, Hot Jupiters

## 1. INTRODUCTION

Thousands of exoplanets have been discovered to date, but each exoplanet detection method is sensitive to specific regimes. This leaves gaps in exoplanet parameter space. In this thesis work, we show that long-baseline optical interferometry can be used to fill two such gaps: 1) the detection of new planets around stars more massive than the Sun (Project ARMADA), and 2) the characterization of known planets that are extremely close to their host star (Project PRIME). Both projects require advanced techniques to push the capabilities of current instruments – either by maintaining precision astrometry, or by measuring ultra-precise closure phases.

Exoplanet detection via the radial velocity (RV) method is extremely difficult for “hot” stars (i.e. early F, A, and B spectral type) due to their weak and broad spectral lines. These stars have also been neglected in most large transit surveys such as Kepler, which had the primary goal of characterizing planets around Sun-like stars. This means that our knowledge of  $\sim 1$  au planet demographics around intermediate mass stars comes largely from studies of cooler, evolved subgiants – “retired A stars.” Ref. 1 and 2 found that there is up to a five-fold increase in the presence of massive gas giant planets in about 1 au orbits compared to solar-type stars. Although this basic result is supported by recent direct imaging work of 3-100 au massive planets observed from Gemini Planet Imager,<sup>3</sup> there is some dispute from a focused RV search of hot stars<sup>4</sup> as well as uncertainty in the progenitor population of the Bowler/Johnson sample.<sup>5,6</sup> We designed an astrometric survey nicknamed ARMADA (ARrangement for Micro-Arcsecond Differential Astrometry) to study this regime by directly observing hot stars for  $\sim$ au-separation gas giant exoplanets. By using one star of a binary system as an astrometric reference, a quick snapshot of interferometry data gives us a precise measurement of the position of one star relative to the other. After monitoring a binary source with a long enough time baseline, we can search for additional “wobble” motions that are caused by companions orbiting either component of the binary.<sup>7</sup> This astrometric signal increases with the planet separation from its host star, making it an ideal method to probe the  $\sim$ au regime around massive stars in binary systems. We’ve demonstrated that the Michigan Infrared Combiner - Exeter (MIRC-X<sup>8</sup>) instrument at the Georgia State University Center for High Angular Resolution (CHARA<sup>9</sup>) array and the GRAVITY<sup>10</sup> instrument at the Very Large Telescope Interferometer (VLTI) array can be used to perform this survey with “hot” stars. We now have a multi-year time baseline on many of the targets in our survey, with enough epochs to probe down to planetary masses. In this manuscript we describe the wavelength calibration steps that need to be taken with the MIRC-X instrument at the CHARA array to maintain precision astrometry, which demanded the implementation of a new etalon module to increase the wavelength precision of this instrument. We also summarize our published detections at CHARA and VLTI and show detection limits for some systems without additional companions.

While Project ARMADA focuses on discovering new exoplanets in a unique regime, long-baseline interferometry can also be used to directly detect the flux from known close-in exoplanets. Hot Jupiters are ideal targets for constraining exoplanet atmosphere models due to their favorable planet-to-star flux ratios compared to other exoplanets. To date, detections of transmitted starlight (transmission spectra) or emitted light from planets (emission spectra) have been made for  $>50$  transiting hot Jupiter exoplanets. Based on these impressive Spitzer, HST, and ground-based results, studies of transiting planets have yielded an abundance of information on their atmospheric characteristics.<sup>11-14</sup> Despite all the exciting progress, key questions, like the diversity of circulation efficiencies and thermal inversion in some planets, are still not fully understood. We introduce a new method for characterizing hot Jupiter planets with long-baseline interferometry. Ground-based long baseline interferometry is already becoming a valuable tool in the field of exoplanet science. The ExoGRAVITY team, for example, is using the GRAVITY instrument at VLTI to directly detect and measure spectra and orbits of planets separated by  $\sim 50-100$  milli-arcsecond (mas) from their host star.<sup>15</sup> This opens up a new parameter space for planet characterization, as these exoplanets are often within the diffraction limit of single telescopes. The CHARA array has an angular resolution of about 0.5 mas in the H-band. This is sufficient to resolve a number of hot Jupiter systems

from their host star, if the high contrast can be achieved. We started a project using the MIRC-X instrument at the CHARA array to measure low-resolution spectra of non-transiting hot Jupiter planets, nicknamed Project PRIME (PRrecision Interferometry with MIRC-X for Exoplanets). The pioneering work for project PRIME was undertaken by Ref. 16. In these efforts, the MIRC instrument at the CHARA array was used to target the hot Jupiter Ups And b. Strict upper limits were placed on the planetary flux at a level of a few times  $10^{-4}$ , only a couple factors away from detecting the expected flux level of the planet in H-band. Since this work, the MIRC instrument has been updated from a 4-telescope combiner to 6-telescopes. It has also undergone multiple optics and detector upgrades to become the current MIRC-X instrument.<sup>8</sup> Recently, the MYSTIC instrument has also been commissioned at the CHARA array to simultaneously record K-band data with MIRC-X.<sup>17</sup> These upgrades have motivated a new attempt to detect the flux from non-transiting hot Jupiter exoplanet Ups And b. If such a detection can be achieved, this would demonstrate a new method for characterizing close-in planets. Along with being a valuable tool for studying non-transiting hot Jupiters, such a tool would also become valuable in the era of Gaia. Gaia is expected to discover hundreds of thousands of new exoplanets,<sup>18</sup> many of which will be too close-in to their host star to resolve with non-interferometric techniques. Though most will likely be too high contrast, long baseline interferometry can be used for some of these companions to measure low resolution spectra in the near-infrared wavelengths.

In Section 2 we give an overview of Project ARMADA. This includes our new wavelength calibration method at MIRC-X/CHARA, a summary of our published triple detections at MIRC-X/CHARA and GRAVITY/VLTI, and our current non-detection limits for systems without an additional companion. In Section 3 we give an overview of Project PRIME to characterize close-in hot Jupiter planets. We describe our self-calibration routine to achieve sub-degree precision in closure phase, and we show promising contrast limits with the MIRC-X and MYSTIC instruments at CHARA. We conclude in Section 4 by giving a look to the future of studying exoplanets with these techniques.

## 2. PROJECT ARMADA FOR EXOPLANET DISCOVERY

Long-baseline interferometry can measure extremely precise differential astrometry of binary stars when both stars are within the field-of-view of the interferometer. Current instruments such as MIRC-X and GRAVITY can measure differential astrometry down to the 10 micro-arcsecond ( $\mu\text{as}$ ) level for close binaries.<sup>10,19</sup> This astrometric precision is sufficient for measuring additional “wobble” motions from previously unseen companions down to the planetary mass regime. Motivated by this precision, we started Project ARMADA as a survey of mostly A/B-type binaries to hunt for additional companions orbiting individual components of the binary system. This is a regime that is difficult to probe with any other method (see Figure 1).

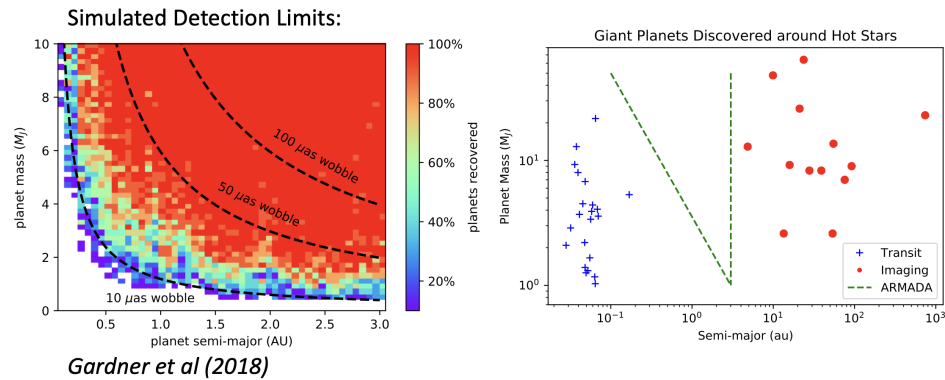


Figure 1. (Left) We inject planets to our MIRC epochs of known binary system  $\delta$  Del in order to estimate our detection limits for additional companions.<sup>19</sup> If we are able to achieve this precision on many binary systems with a survey, we can fill the  $\sim 1$  au gap around main-sequence A/B-type stars (Right). This regime is extremely difficult to probe with other methods.

## 2.1 Wavelength Calibration at the CHARA Array

In Ref. 19 we demonstrated with the close ( $<10$  mas) binary system  $\delta$  Del that the MIRC instrument at the CHARA Array was achieving precision sufficient for recovering Jupiter mass planets on  $\sim$ au orbits around individual components of the binary system. However, in practice we need to probe wider binary systems than this in order to minimize the suppression of planets due to the influence of a close binary companion.<sup>20</sup> In the high resolution modes for MIRC-X and GRAVITY-ATs, the field-of-view of the interferometer is about 200 mas. Hence our goal is to maintain  $10\ \mu$ as differential astrometry for binaries out to these separations. However, many error terms scale with the separation of the binary. For the 10 mas binary  $\delta$  Del, we achieved  $1e-3$  relative precision with our  $10\ \mu$ as residuals. For a 100 mas binary, this relative precision needs to be at the  $1e-4$  level. This means maintaining wavelength calibration between ARMADA nights at this precision. For GRAVITY/VLTI, the quoted wavelength precision in high resolution mode is at the  $\sim$ 5e-5 level using the Fourier Transform Spectrometer.<sup>21</sup> For MIRC-X/CHARA, however, the quoted precision is at the  $1e-3$  level,<sup>8,22</sup> too high for exoplanet work using astrometry of wide binaries.

To improve the wavelength precision at MIRC-X/CHARA, we implemented a new calibration technique to bring our precision to at least the  $1e-4$  level between ARMADA nights. We designed and installed a custom-made module of six etalons (one for each of CHARA's telescopes) enclosed in a thermally stable holder which is placed into the beam path each ARMADA night for additional calibration. These etalons produce a similar signal to a binary star, but one where we know precisely the separation (since we know the thickness of each etalon). Thus, we can monitor how our wavelength solution varies from night-to-night when etalon data is taken. Ref. 7 fully describes our models and fitting techniques to this data, and we show some example data in Fig. 2.

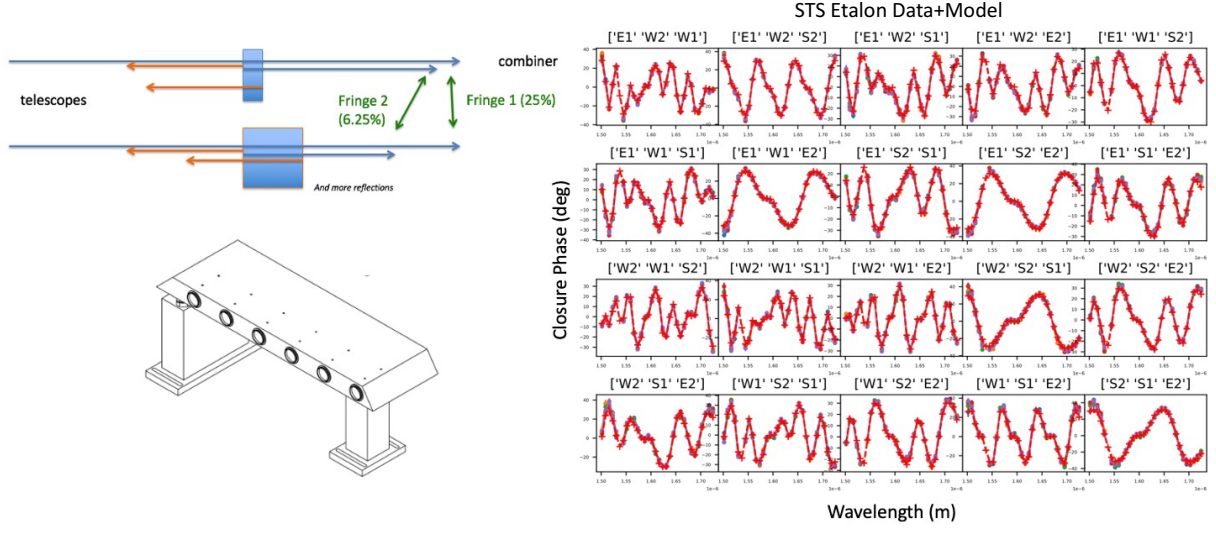


Figure 2. In order to maintain  $\sim$ 10  $\mu$ as astrometry on wider binaries, we needed to improve the wavelength calibration precision at MIRC-X/CHARA. We implemented a set of 6 etalons of different thickness in a thermally stable holder to simulate the signal of a binary star of known separation. By taking data with the etalon each ARMADA night, we can monitor how the wavelength solution is varying from night-to-night and bring all of our data to the same internally accurate astrometric scale. We take data at least once per night, now with the lab light source Six Telescope Simulator (STS). We show an example snapshot of this etalon data. Each measurement gives closure phases for each of MIRC-X's 20 closing triangles with 6 telescopes. It is hard to distinguish between the model fit in red and the data in blue.

We now have etalon data taken for the ARMADA program spanning over 3 years from late 2017 - 2021. Each night the etalon data is turned into a “scale factor” which we apply to our astrometry measurements for that night. We set one high SNR etalon night as a reference (i.e. scale factor of 1.0), and compute how the wavelength solution changes compared to the reference as described in Ref. 7. Fig. 3 shows how this scale factor varies across over 100 nights. When the MIRC-X instrument was first implemented there were large jumps due to detector and optics upgrades, and a changing of the readout window on the detector for fringes. Since then, the solution

has been more stable with maximum etalon variation at the  $1e - 3$  level. By testing this etalon wavelength scheme on a known test source, we verify that our calibration has improved the wavelength precision.<sup>7</sup>

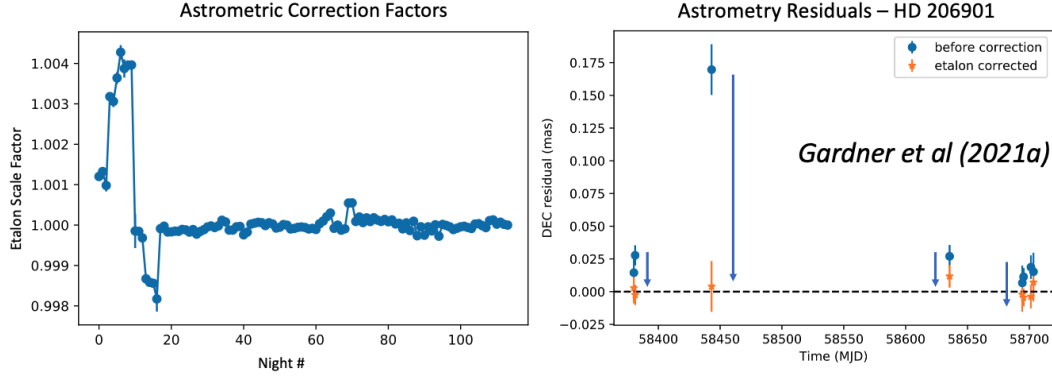


Figure 3. (Left) We use the etalon data to compute an astrometric correction factor for each ARMADA night, based on a reference night. This makes all of our MIRC-X/CHARA data internally consistent. Large jumps toward the beginning of ARMADA are due to MIRC-X detector and optics upgrades, and a change in the detector readout windows. Since then, the wavelength solution has been more stable. (Right) We demonstrate on a test source  $\kappa$  Peg that our etalon calibration scheme is indeed working to allow us to measure  $\sim 10 \mu\text{as}$  astrometry on wide (up to 200 mas) binaries.

## 2.2 Newly Detected Triple Stars

Although our ultimate goal for ARMADA is to search for planets around A/B-type binaries, the first objects that we are detecting are previously unseen triple stars. When there is an additional stellar companion orbiting one component of an ARMADA binary, the “wobble” signal is much larger compared to a planet. Hence our ARMADA survey is essentially 100% complete for inner stellar mass companions. In Ref. 7 and Gardner et al (2022, submitted), we published the orbits of 15 triple systems – most of which were first detections of the inner subsystem. In Figure 4 we demonstrate how our search routine works to uncover previously unseen additional companions. We use historical data from the Washington Double Star (WDS) Catalog to constrain the long period outer binary orbit along with our new ARMADA epochs. We then perform a grid search over inner orbital period to search for a third body in the system (simultaneously re-fitting the outer binary at each step). We are also performing RV follow-up of these newly detected triples both to confirm the orbital period and to deduce which star the new companion is orbiting (Gardner et al 2022, submitted). Our survey has proven to be extremely successful at detecting previously unknown inner stellar components, with median residuals to the triple fits at a few tens of micro-arcseconds (varying from 10–50  $\mu\text{as}$  in published orbits). For binaries of separation range 50–200 mas, this means we are achieving relative precision at the 0.5–2e-4 level with our observational setups at CHARA and VLTI.

## 2.3 Detection Limits

For targets without a confident detection of an inner component, we are able to set upper limits. We follow the procedure outlined in Ref. 19 for computing detection limits. We inject companion signals to our data on a grid of companion orbital period and “wobble” semi-major axis. This is then converted to companion mass, given our estimates of the distance (from Hipparos or Gaia) and stellar masses (from spectral type). At each point of this grid, we simulate 1000 circular planets with randomly chosen values for the other orbital elements. We then use the same routine applied to the science data to fit for the injected planet + binary orbit over this grid. We record how many of the 1000 planets we are successfully able to recover at each grid point. Since the  $\chi^2$  statistic cannot be used to compare models with a different number of free parameters, we use the Bayesian Information Criteria (BIC) to determine whether or not our triple fit is better than the binary fit. This criteria is also commonly used to claim RV planet detections.<sup>23–25</sup> The BIC is computed by

$$BIC = -2 \ln \mathcal{L} + k \ln n, \quad (1)$$

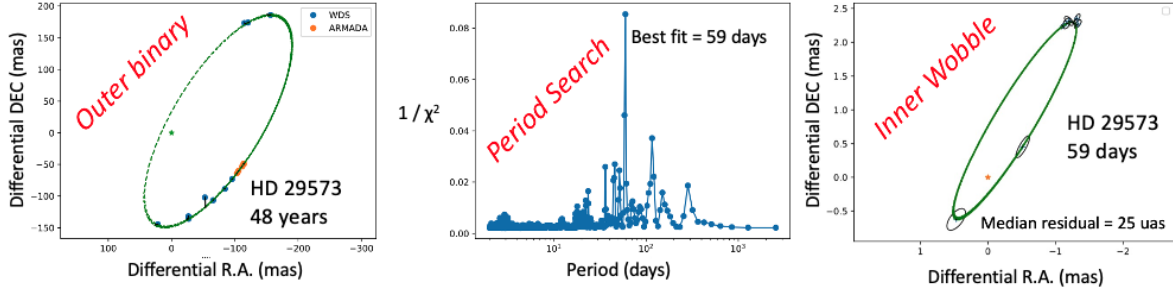


Figure 4. (Left) Since our ARMADA epochs only cover a small arc of the outer binary orbit, we constrain the outer orbit with historical data from the WDS catalog. (Center) Starting from our best-fit of the outer binary orbit, we grid search over inner orbital period for additional companions. Here there is a newly detected companion with a 60-day orbital period. (Right) We subtract out the outer binary motion to show the inner “wobble” motion due to the previously unseen inner companion.

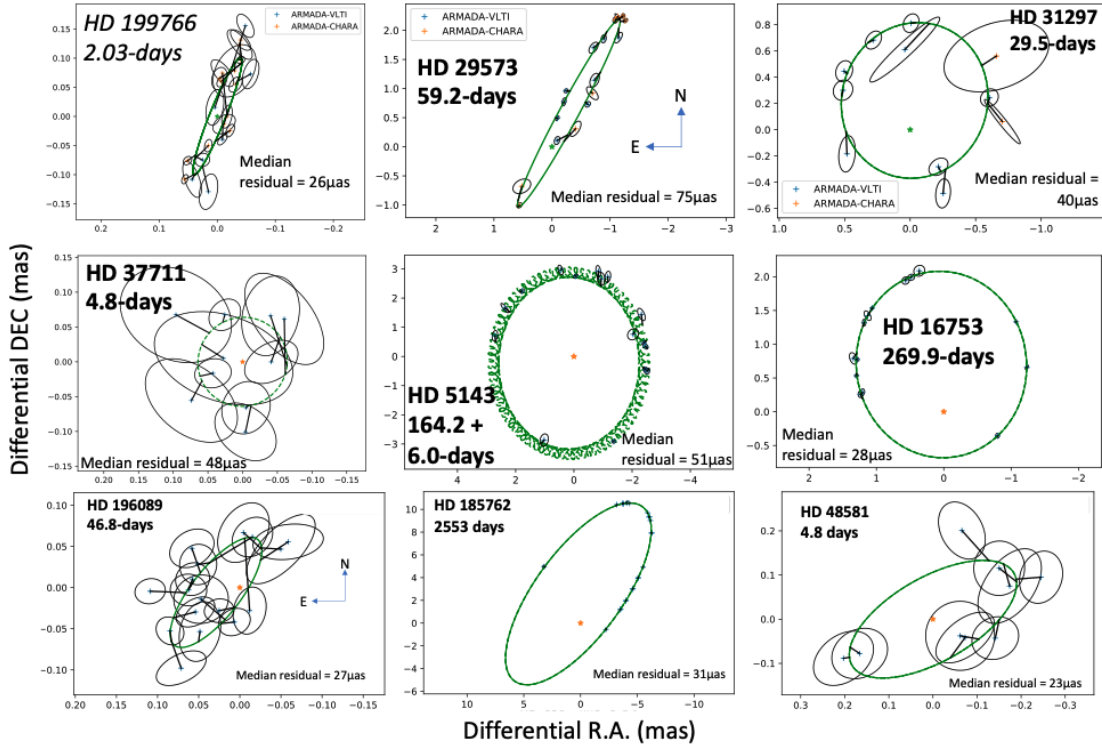


Figure 5. We show some example inner “wobble” orbits from newly detected stellar mass components to ARMADA binaries at both MIRC-X/CHARA and VLTI/GRAVITY. The top row shows three systems with data combined from both instruments. Note that we are uncovering “wobble” motions at  $<100 \mu\text{as}$  in some cases here, with median residuals to the triple fit usually within 20–50  $\mu\text{as}$ . HD 5143 is a newly detected quadruple system, so its inner orbit as a “wobble” motion of its own. All triples are published in Ref. 7 and in Gardner et al (2022, submitted).

where  $k$  is the number of free parameters,  $n$  is the number of data points, and  $\mathcal{L}$  is the likelihood function. For our models,  $-2 \ln \mathcal{L} = \chi^2$ . The model with a lower BIC value is selected as being a better fit to the data. To accept a triple model as a better fit, we require  $\Delta \text{BIC} > 5$  and also check that the recovered companion period and semi-major axis are within 30% of the true injected value.

Each point on our grid records the percentage of injected companions which we are able to successfully recover. For each target we plot contour lines that show the region above which we could have recovered 10%,

60%, or 99% of companions at a given mass and orbital period. As can be seen in the example system in Figure 6, we are able to probe down to the few Jupiter-mass regime for a number of our targets at 300-day orbital periods (the  $\sim$ au range). For that case of A-type binary HD10453, we can rule out a tentative detection of a 31.1  $M_{Jup}$  companion reported in the high precision RV work of Ref. 4. We show a histogram for non-detection limits for 20 binaries in our sample with  $N_{epoch} > 10$  in Figure 7. These limits depend not only on orbital precision achieved at CHARA, but also on the mass of the host star and the system distance. Since we include B-type stars in our survey, it is harder to probe down to a Jupiter mass for these targets as well as for those at a further distance.

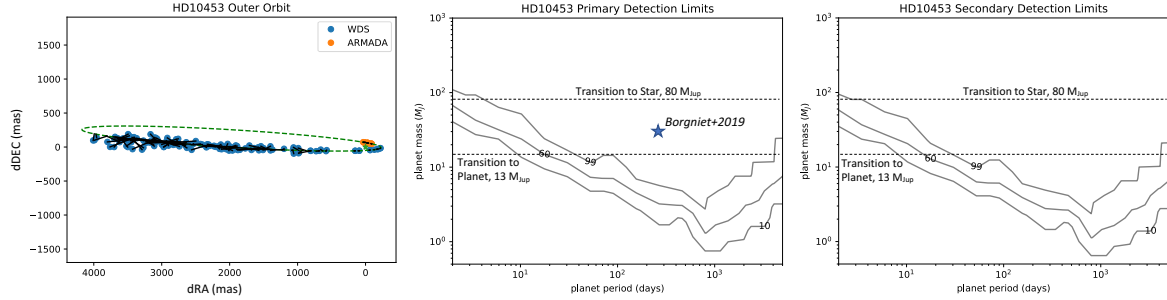


Figure 6. To compute detection limits in cases without a candidate companion detection, we simulate planets on a grid of planet period and mass. We report the contour lines where we recover 99%, 60%, and 10% of injected companions. Since each binary pair consists of two stars, we are able to rule out a detection around both components. (Left) we show the outer binary orbit of A-type binary HD10453, using historical WDS data combined with our new ARMADA epochs. (Center and Right) We show the non-detection limits for additional companions orbiting individual components of the binary pair. The horizontal lines depict  $80 M_{Jup}$  (transition to substellar) and  $13 M_{Jup}$  (transition to planet). We can rule out a tentative detection of a companion around the primary with minimum mass of  $31.1 M_{Jup}$  reported with high precision RV in Ref. 4.

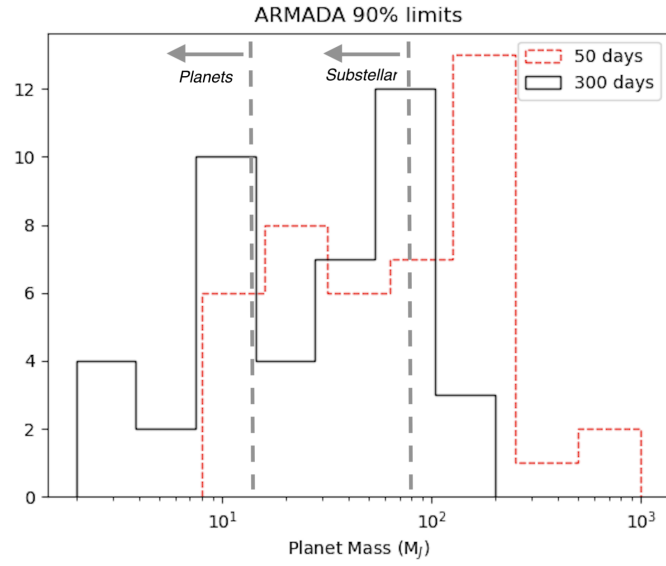


Figure 7. We show histograms of our 90% confidence limits for ARMADA binaries with sufficient epochs at 50 and 300 day orbital periods. We are probing the substellar regime ( $< 80 M_J$ ) at  $\sim$ au orbits for most of these targets, and we can reach planet masses for the lower mass or closer systems in the sample. However, we need improved astrometry to reach the Jupiter mass regime for most targets.

### 3. PROJECT PRIME FOR EXOPLANET CHARACTERIZATION

Ground-based long baseline interferometry is a potentially powerful tool for characterizing exoplanets which are too close to their host star to be imaged with classical single-dish telescopes. The CHARA array achieves resolutions down to 0.5 mas for the longest baselines, allowing us in principle to directly measure the near-infrared spectra of close-in exoplanets down to this limit, if the required high contrast can be achieved. We have started a project using the MIRC-X instrument at the CHARA array to measure low-resolution spectra of non-transiting hot Jupiter planets, nicknamed Project PRIME. The first hot Jupiter that we targeted for this program is Upsilon Andromedae b.

In order to explore the contrast levels we need to achieve with MIRC-X and MYSTIC, we use updated global circulation models (GCMs) for Ups And b's atmosphere to compute model spectra. Ref. 26 recently computed GCMs for Ups And b, using the models described in Ref. 27 and 28. The values assumed for Ups And b matched those of recent high precision spectroscopy work of Ref. 29, with a planet mass of  $1.7 M_{Jup}$ . The orbital period was set to 4.617 days, semi-major axis 0.0595 au, orbital inclination of  $24^\circ$ , stellar effective temperature of 6212 K, and stellar radius of  $1.0296 \times 10^9$  meters (these choices are justified in Ref. 26). These authors reported model spectra as a function of orbital phase in their paper, though the wavelength regime did not match our observations. We extended these spectra to the H and K band, for both their clear and cloudy models of the hot Jupiter atmosphere. We show the updated model spectra in Figure 8. These spectra demonstrate that we need to measure contrasts of  $\sim 2e-4$  in the H-band ( $\sim 4e-4$  in K-band) in order to detect the planet. If successful, we can also measure how the low resolution spectra changes across the orbit of the planet.

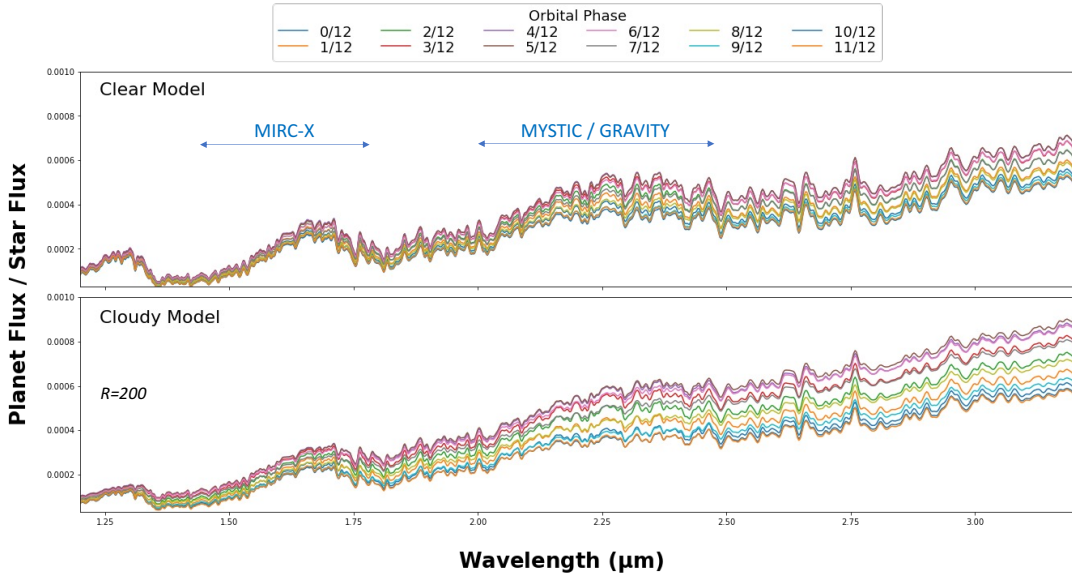


Figure 8. We use the GCMs of Ref. 26 to produce model spectra dependent on orbital phase for Ups And b spanning the H and K bands, for both a clear and cloudy atmosphere case. If we can achieve contrasts of  $2e-4$  in H-band, or  $4e-4$  in K-band, we will be able to constrain hot Jupiter GCMs by measuring low resolution spectra across the orbit of the planet.

#### 3.1 Observations and Data Reduction

Data for PRIME are taken in H-band grism mode ( $R \sim 190$ ) with the MIRC-X instrument at the CHARA Array. Here we present early results from data taken in 2021 October (4 nights), which includes data with the newly commissioned MYSTIC instrument.<sup>30,31</sup> MYSTIC takes data in the K-band, and is used simultaneously with MIRC-X. For K-band MYSTIC, we used the prism  $R \sim 50$  mode. Since Ups And is a bright star ( $H=3.0$ ) that is only resolved on the longest baselines ( $UD=1.097$  mas), this is a relatively simple target to observe with

MIRC-X/MYSTIC. The challenge of this program comes in achieving the SNR and closure phase precision to be able to detect the flux from the planet which is at an expected level of contrast approaching 5,000:1. Normally, interferometric observations employ frequent pointings to calibrator stars (sources with known sizes). This allows one to calibrate losses in the visibility due to atmospheric or systematic effects. For our program we are attempting to detect the hot Jupiter in the closure phase signal, which is immune to atmospheric effects. Ref. 16 showed that the level of precision needed to detect Ups And b in the closure phase is at the  $\sim$ 0.1 degree level in H-band. At this level, we detect systematic features in closure phase across the night which need to be calibrated. Though we observed some calibrators on these nights, we find that the target data itself is best for modeling closure phase systematics (since Ups And is bright and we spent most of the night on-target, our closure phase precision is significantly better compared to shorter calibrator pointings). We describe our self-calibration routine in the next section, and note that future runs will drop pointings to calibrators altogether so that we can spend as much time as possible integrating on target.

We use the MIRC-X pipeline (version 1.3.3, which also reduced MYSTIC data) to produce OIFITS files for each night.<sup>8</sup> At this stage, we do not yet carry out any calibration of our target data. So the closure phase and visibility that the pipeline measures will be raw (i.e. uncalibrated). Since we take extra cleaning and calibration steps for project PRIME, we want short integrations of closure phase at this step which will be averaged together at a later step. Hence we reduce our data with an oifits max integration time of 30 seconds, and a number of coherent integration frames (ncoh) of 10. We also apply the bispectrum bias correction of the pipeline. After obtaining our 30-second chunks of closure phase measurements across a night, we then clean up our data with an IDL routine specially made for this program. This routine follows the principles described in Ref. 22 for the MIRC pipeline, which was well tested to flag and remove bad data and average together closure phase and visibility. This script then cleans the data by removing outliers and averages the closure phase measurements into 15-minute chunks. For MYSTIC, we now have clean datasets with 7–9 spectral channels for the R $\sim$ 50 mode. Our MIRC-X data is taken with a higher resolution, so we perform a median filter across wavelength to average our data from  $\sim$ 34 spectral channels to 7–9 channels. At this step we now have cleaned and averaged closure phases for each night, though these measurements are still uncalibrated.

### 3.2 Self-Calibration for Achieving Precision Closure Phase

At this stage, our closure phase precision is already at the sub-degree level in standard deviation across time and triangles for both MIRC-X and MYSTIC. However, we do see systematic features in the closure phase which are not from the hot Jupiter planet. Fig. 9 shows MYSTIC closure phase data across time for one spectral channel during the night of 2021Oct21. As can be seen, there are clear drifts with time and some odd “dips” in the closure phase signal. These need to be calibrated out in order to detect any signal from a hot Jupiter planet. It is especially worthy to note that multiple triangles share a strong “dip” feature as the source is transiting (i.e. passing through its highest point) in the sky. This potentially hints at a polarization issue which is affecting our data at a sub-degree level.

Ref. 16 described a calibration model which greatly improved the precision of MIRC data on Ups And b. In that work, the authors used calibrator sources to model closure phase behavior as a function of altitude and azimuth of the target in the sky. However, the expected closure phase signal from the hot Jupiter exoplanet does not follow these trends with altitude and azimuth. And hence we can use the target data itself to model these systematic effects. This way we do not need to extrapolate the model into regions where there is no calibrator data, and we have higher precision data to model such effects since more time is spent on the bright, high SNR target star. Additionally, it means that we are able to integrate on-target all night which increases our coverage and signal for the extremely faint hot Jupiter companion. We find the following model to best describe the systematic features in closure phase with altitude and azimuth:

$$\phi = a_0 + a_1 * Az + a_2 * Az^2 + a_3 * Az * Alt + a_4 * Alt + a_5 * Alt^2, \quad (2)$$

where  $\phi$  is the closure phase signal due to systematic drifts,  $a_n$  are fitted coefficients, and Az and Alt refer to the target azimuth and altitude.

### HD 9826, Closure Phase, Channel 3

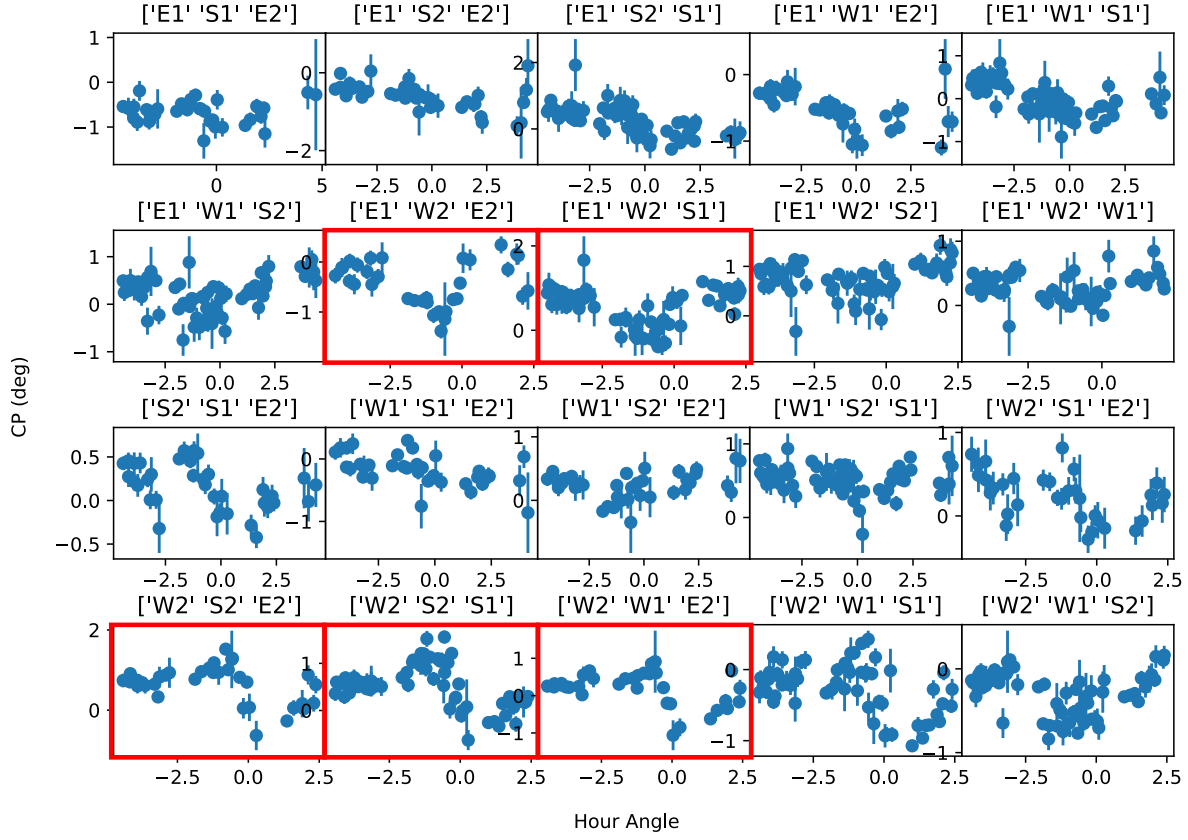


Figure 9. We plot the MYSTIC closure phase for one spectral channel across hour angle during the observing run of 2021Oct. Each box represents one of the 20 closing triangles of the CHARA array. Though we are already looking at sub-degree features, the drifts and dips need to be calibrated out in order to reach the precision needed to detect the flux from a planet. Five triangles are highlighted in particular to show strong drops in closure phase, which happen to occur as the source Ups And is passing through its highest point in the sky.

We use the model of Equation 2 to fit for each spectral channel separately, and combine all the nights of a single run together to fit for the coefficients per spectral channel. Figure 10 shows our model fit on a select few triangles. We are able to capture many of the drifts with our model of altitude and azimuth, which increases the closure phase precision for both instruments. Once we subtract out these systematics from the target closure phase data, we are ready to search for the flux from the hot Jupiter planet.

### 3.3 Grid Search Routine

Once we have our final reduced, cleaned, and self-calibrated closure phase data, we can begin to search for the signal from the high contrast planet. To do so, we fit a Keplerian orbit model directly to the closure phases. All nights from a single run are fit simultaneously. The orbital elements for a planet/binary orbit consist of an orbital period  $P$ , a semi-major axis  $a$ , an inclination  $i$ , an eccentricity  $e$ , the longitude of periastron  $\omega$ , the position angle of the ascending node  $\Omega$ , and the time of passage through periastron  $T$ . For a given observation time these orbital elements will predict the position ( $\Delta x$ ,  $\Delta y$ ) of a companion relative to the primary star at the origin. The closure phase signal is then set by this position, along with a flux ratio  $f = f_{\text{star}}/f_{\text{planet}}$ , and a uniform disk (UD) size for the primary star and planet. Hence we can fit to our data with the binary orbital elements, planet/star contrast, and uniform disk size of Ups And as free parameters.

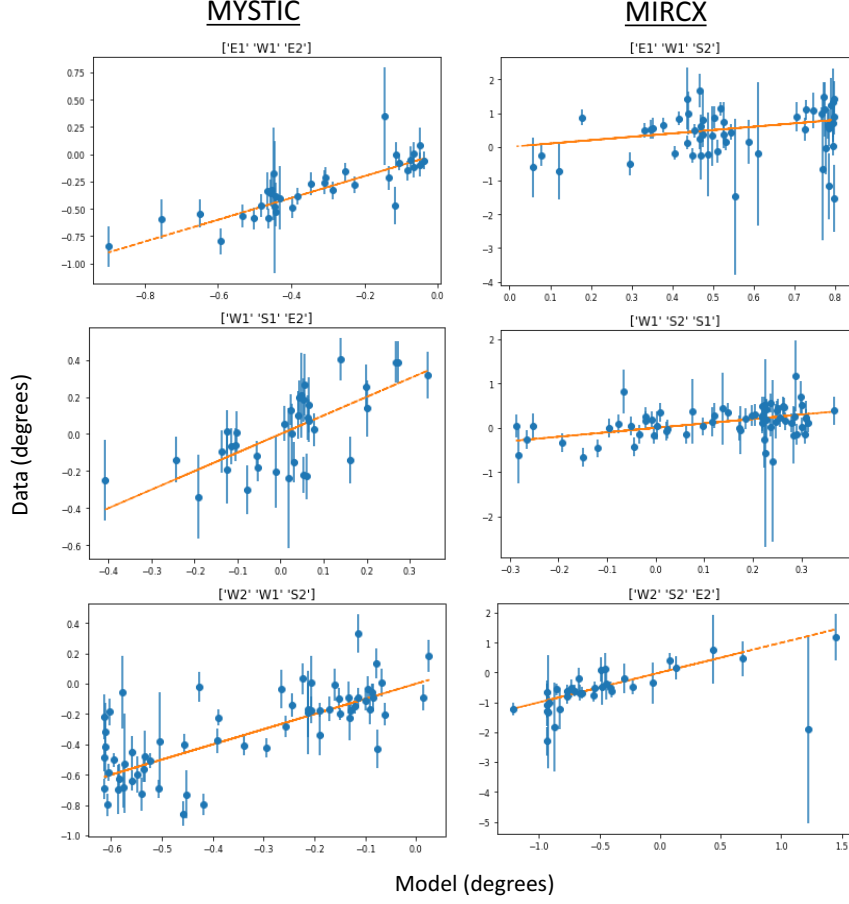


Figure 10. We show our model vs. data fits for the 2021Oct shared MYSTIC (left column) and MIRC-X (right column) runs. We are plotting a single spectral channel, for three triangles of each instrument. Our model fits for the coefficients in Equation 2 to calibrate out systematic drifts in closure phase with altitude and azimuth. As mentioned in the text, we use our target data itself for self-calibration. While most of these trends are at the sub-degree level, our model does indeed capture some of the closure phase drifts to increase our precision.

Ups And b has been characterized in RV, which provides many of the known orbital elements of the planet. Ref. 29 most recently published an updated RV orbit for this planet, and hence we are able to use these values to inform our searches. We fix  $P = 4.617111$  days,  $e = 0.012$ ,  $\omega = 224.11^\circ$ , and  $T = 50033.55$  MJD from the fitted values to the RV data for Ups And b. We also set the host star  $UD = 1.097$  mas,<sup>16</sup> and we keep the planet size unresolved at 0.1 mas. Hence our free parameters are then  $a$ ,  $i$ ,  $\Omega$ , and  $f$ . However, since we know the mass of the star ( $1.31 \pm 0.02 M_\odot$ <sup>29</sup>), the orbital period, and the distance to the system ( $13.48 \pm 0.04$  pc,<sup>32</sup>) we also have a good estimate of the orbital semi-major axis:  $a = 4.4$  mas. We also note that Ref. 29 reported the orbital inclination of Ups And b to be  $24 \pm 4^\circ$ . However, this value is not as reliable as the others, since it depended on the detection of water vapor in the atmosphere of the planet which Ref. 33 calls into question based on simulations of these features which suggest that it should not have been detectable. To search for the planet we perform a brute force grid search over the parameters of  $a$ ,  $i$ , and  $\Omega$ , letting the flux ratio  $f$  vary as a free parameter at each step. We vary  $a$  from 3–6 mas at a step size of 0.1 mas (later, we fix it as a free parameter at the known value of 4.4mas),  $i$  from 0–180° at a step size of 3°, and  $\Omega$  from 0–360° at a step size of 2°. We then look for the minimum  $\chi^2$  location to find the location of the planet, plotted in the next section as heat maps. We use the Python package *lmfit*<sup>34</sup> to perform our  $\chi^2$  minimization at each step of the grid (note that only the flux ratio varies as a free parameter at each step).

### 3.4 Ups And b – MIRC-X and MYSTIC Injection Tests

To test whether or not our self-calibration routine is working, we first inject a planet signal into the raw closure phase of our MIRC-X and MYSTIC data. This injected planet has the RV orbital elements described previously, and we added this planet at an inclination of  $24^\circ$  and an  $\Omega$  of  $51^\circ$ . We then ran our data through the cleaning and self-calibration pipelines described above, to see whether or not we could recover the signal from injected planets of varying contrasts. Figure 11 shows the results of these tests. As can be seen, with MIRC-X the injected planet is recovered at the expected position at contrast levels down to  $2e-4$ . For MYSTIC data we successfully recover the best-fit location for contrasts of  $4e-4$  and  $3e-4$ , though it is still visibly present down to  $2e-4$  (if combined with a MIRC-X detection, this would be quite convincing). Although we recover the correct position in most cases, the fitted contrast is not always equal to the injected contrast. This could be due to complications from the real planet signal itself, which is expected to be present in our data. Future work will dedicated to recovering the flux from Ups And b in these datasets and others. If successful, we will be able to use our detections to constrain the spectra in Fig. 8. Our injection tests suggest we are now reaching the contrasts necessary to make such a detection with MIRC-X and MYSTIC.

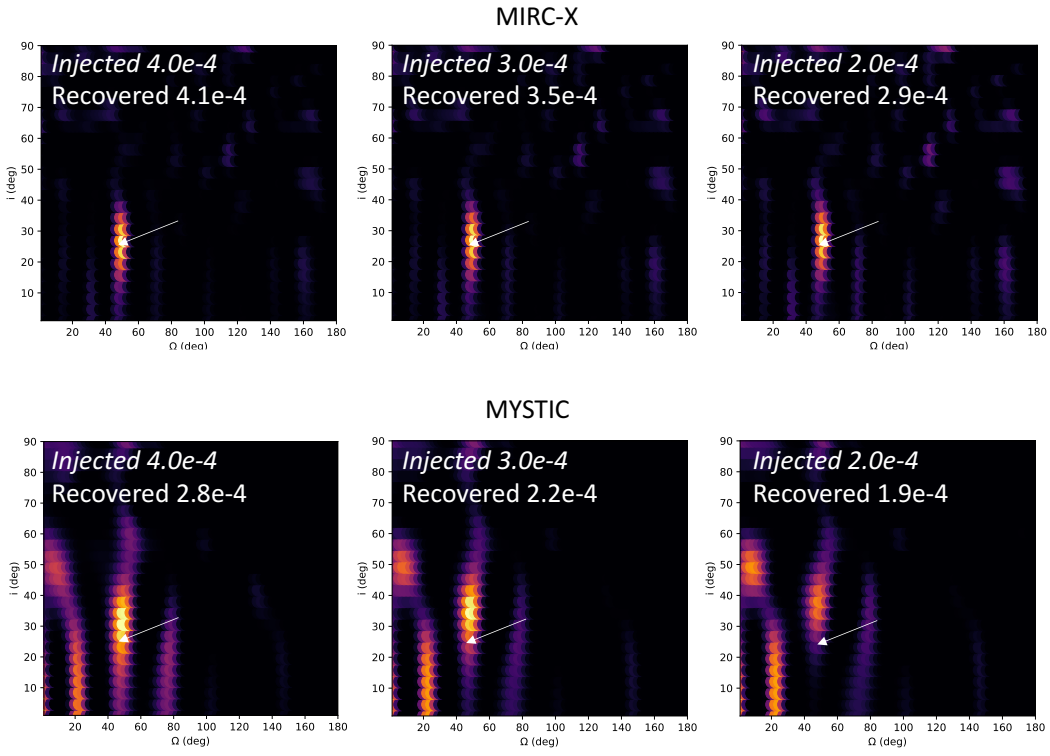


Figure 11. In order to test our self-calibration routine and explore MIRC-X and MYSTIC contrast limits, we inject planet signals to our 2021Oct dataset at the predicted location of Ups And b for varying star/planet contrasts. The arrows point toward the injected location in these  $\chi^2$  heat maps. We successfully recover the planet down to a contrast of  $2e-4$  with MIRC-X, and we can see the planet signal at this contrast for MYSTIC. Our recovered contrast values do not always match the injection, which could be a sign that we are seeing some signal from the true planet.

## 4. CONCLUSIONS

Long baseline interferometry is a powerful technique for studying exoplanets in regimes that are off-limits to instruments on single-dish telescopes. We developed two techniques to probe unique regimes of exoplanet science. Project ARMADA utilizes the incredible astrometric precision in differential measurements of binary stars with MIRC-X/CHARA and GRAVITY/VLTI in order to search for companions down to planet masses, while Project

PRIME aims for precision closure phase measurements at MIRC-X/CHARA in order to directly detect the flux from non-transiting hot Jupiters.

In Sec 2 we described our methods for maintaining  $\sim 10$ s  $\mu$ as astrometry over multiple years on binary systems separated by up to 200 mas. This is challenging in practice, since systematic errors in differential astrometry scale with the separation of the binary. The MIRC-X instrument at the CHARA array reports a nominal  $\sim 1$ e-3 error in precision, and we need to achieve at least 1e-4 precision for 100–200 mas binaries. We implemented a wavelength calibration scheme with MIRC-X at the CHARA array to maintain astrometric precision at the few tens of micro-arcsecond scale, which is about an order of magnitude better than what is achievable without such calibration at CHARA. This work has also led to the publication of some of the most precise astrometric binary and triple orbits in the field. We have published 15 previously unseen companions of stellar mass in our ARMADA binary sample. Many of these inner “wobble” motions from new companions are at the  $< 1$  mas level, demonstrating the incredible precision possible with this method. We also show that we are probing the substellar mass regime for a number of our ARMADA binary targets without detections, though our method still struggles to reach down to 1 Jupiter mass. This is particularly true for the more massive and further out systems in our sample, where precision  $< 10$  micro-arcseconds is needed to detect such planets. This precision will not soon be achieved by other methods either. The Gaia mission will be the closest to achieving such astrometric precision for intermediate mass stars, with expected single-epoch precision of 50  $\mu$ as by the end of its 5-year mission. Ref. 35 predicts that Gaia may have the precision to detect  $1 M_J$  planets around A-stars within 20 pc, though this is still uncertain due to the brightness of the sources. In any case, this does not leave a large amount of intermediate mass stars for Gaia to find lower mass planets. Since our goal is to detect  $\sim 1 M_J$  planets at the au-regime around A/B-type stars, every improvement that can be made to the astrometric precision at CHARA and VLTI is crucial to get closer to achieving this goal. The most likely culprit currently limiting our astrometry of 200 mas binaries is the control of the starlight pupils. As described in Ref. 36, aberrations or shifts in the pupil injection can result in errors which effectively amount to measuring the incorrect length for the interferometer baseline. Just as required for wavelength precision, our baseline knowledge must also be known better than 1e-4 for 10  $\mu$ as astrometry of a 100mas binary. With adaptive optics now implemented at VLTI, and partially implemented at CHARA, the control of the pupils should be improving with time. Unfortunately, we did not have a way to reliably monitor this across our ARMADA survey. Future instruments at CHARA such as SPICA will monitor the pupil injection, and there are efforts planned to carry out such monitoring with MIRC-X as well with the upcoming STST pupil monitor. A worthwhile future study would be to test how pupil injection affects astrometry, and to perhaps monitor or correct for such shifts in order to probe down to  $< 10$   $\mu$ as differential astrometry.

In Sec 3 we described our continuing efforts to use interferometry for characterizing close-in exoplanets. Ref. 16 pioneered the efforts to use the CHARA array to directly detect the H-band spectrum of non-transiting hot Jupiter Ups And b. Since that work MIRC was upgraded from 4 telescopes to using all 6, and its detector and optics were upgraded to the current MIRC-X instrument. The MYSTIC instrument was also recently commissioned to take data in the K-band simultaneously with MIRC-X. We obtained 4 nights of data on this system in 2021 October with both MIRC-X and MYSTIC. To achieve the precision needed for a detection, we modeled closure phase systematics across sky position. We developed a self-calibration method which uses the target data itself, and verified that our method was recovering the correct signal with injected planets. We were able to recover an injected planet signal down to 2e-4 contrast for MIRC-X. We could still see the planet signal at this contrast with MYSTIC, though it was no longer the preferred solution. These contrasts are already a remarkable achievement from ground-based long baseline interferometers. Only the recent work of Ref. 15 has demonstrated such high contrast detections at  $\sim 100$  mas with the GRAVITY instrument at VLTI, and this contrast has never been achieved for a  $< 5$  mas companion like Ups And b. We produced up-to-date model spectra for Ups And b as a function of its orbital phase. These spectra demonstrate the type of constraints that our data could place on global circulation models for non-transiting hot Jupiters. As expected, the K-band contrast was always more favorable than the H-band for these types of planets. This makes our method desirable for K-band instruments like GRAVITY and MYSTIC, particularly when combining results from an H-band instrument like MIRC-X. Future work and follow-up observations will focus on searching for the signal from the true planet, and constraining hot Jupiter GCMs if successful. We note that there is a sudden drop in closure phase on multiple baselines as the observed object is transiting in the night sky. This is likely a sign of polarization effects from

interference optics, and hence it can potentially be modeled if we understand the polarization behavior of our beam train. Modeling polarization effects is a major goal of upcoming work on MIRC-X and MYSTIC, and carrying out such efforts will surely help Project PRIME in the future. We demonstrated that contrasts down to 2e-4 at <5 mas can be reached by combining multiple nights of data with current instruments. This contrast is already promising for follow-up of brown dwarfs and planets that Gaia will detect in astrometry. Many such detections will require interferometric techniques for follow-up characterization, since many will be at separations too close to the host star to probe with single dish telescopes.

## ACKNOWLEDGMENTS

T.G. and J.D.M. acknowledge support from NASA-NNX16AD43G and from NSF-AST2009489. T.G. acknowledges support from Michigan Space Grant Consortium, NASA grant NNX15AJ20H. Astronomy at Tennessee State University is supported by the state of Tennessee through its Centers of Excellence program. This work is based upon observations obtained with the Georgia State University Center for High Angular Resolution Astronomy Array at Mount Wilson Observatory. The CHARA Array is supported by the National Science Foundation under Grant No. AST-1636624 and AST-2034336. Institutional support has been provided from the GSU College of Arts and Sciences and the GSU Office of the Vice President for Research and Economic Development. MIRC-X received funding from the European Research Council (ERC) under the European Union's Horizon 2020 research and innovation programme (Grant No. 639889). JDM acknowledges funding for the development of MIRC-X (NASA-XRP NNX16AD43G, NSF-AST 1909165). Based on observations collected at the European Southern Observatory under ESO large programme 1103.C-0477. S.K. acknowledges support from ERC Consolidator Grant (Grant Agreement ID 101003096) and STFC Consolidated Grant (ST/V000721/1). The research leading to these results has received funding from the European Research Council (ERC) under the European Union's Horizon 2020 research and innovation program (project UniverScale, grant agreement 951549). This research has made use of the Jean-Marie Mariotti Center SearchCal service\*. This research has made use of the Jean-Marie Mariotti Center **Aspro** service †. We thank Nuria Calvet for supporting funds in the development of our etalon wavelength calibration module. This research has made use of the Washington Double Star Catalog maintained at the U.S. Naval Observatory. This work has made use of data from the European Space Agency (ESA) mission *Gaia* (<https://www.cosmos.esa.int/gaia>), processed by the *Gaia* Data Processing and Analysis Consortium (DPAC, <https://www.cosmos.esa.int/web/gaia/dpac/consortium>). Funding for the DPAC has been provided by national institutions, in particular the institutions participating in the *Gaia* Multilateral Agreement.

## REFERENCES

- [1] Bowler, B. P., Johnson, J. A., Marcy, G. W., Henry, G. W., Peek, K. M. G., Fischer, D. A., Clubb, K. I., Liu, M. C., Reffert, S., Schwab, C., and Lowe, T. B., "Retired A Stars and Their Companions. III. Comparing the Mass-Period Distributions of Planets Around A-Type Stars and Sun-Like Stars," **709**, 396–410 (Jan. 2010).
- [2] Johnson, J. A., Aller, K. M., Howard, A. W., and Crepp, J. R., "Giant Planet Occurrence in the Stellar Mass-Metallicity Plane," **122**, 905–915 (Aug. 2010).
- [3] Nielsen, E. L., De Rosa, R. J., Macintosh, B., Wang, J. J., Ruffio, J.-B., Chiang, E., Marley, M. S., Saumon, D., Savransky, D., Ammons, S. M., Bailey, V. P., Barman, T., Blain, C., Bulger, J., Burrows, A., Chilcote, J., Cotten, T., Czekala, I., Doyon, R., Duchêne, G., Esposito, T. M., Fabrycky, D., Fitzgerald, M. P., Follette, K. B., Fortney, J. J., Gerard, B. L., Goodsell, S. J., Graham, J. R., Greenbaum, A. Z., Hibon, P., Hinkley, S., Hirsch, L. A., Hom, J., Hung, L.-W., Dawson, R. I., Ingraham, P., Kalas, P., Konopacky, Q., Larkin, J. E., Lee, E. J., Lin, J. W., Maire, J., Marchis, F., Marois, C., Metchev, S., Millar-Blanchaer, M. A., Morzinski, K. M., Oppenheimer, R., Palmer, D., Patience, J., Perrin, M., Poyneer, L., Pueyo, L., Rafikov, R. R., Rajan, A., Rameau, J., Rantakyrö, F. T., Ren, B., Schneider, A. C., Sivaramakrishnan, A., Song, I., Soummer, R., Tallis, M., Thomas, S., Ward-Duong, K., and Wolff, S., "The Gemini Planet Imager Exoplanet Survey: Giant Planet and Brown Dwarf Demographics from 10 to 100 au," **158**, 13 (July 2019).

\*available at [http://www.jmmc.fr/searchcal\\_page.htm](http://www.jmmc.fr/searchcal_page.htm)

†Available at <http://www.jmmc.fr/aspro>

[4] Borgniet, S., Lagrange, A.-M., Meunier, N., Galland, F., Arnold, L., Astudillo-Defru, N., Beuzit, J.-L., Boisse, I., Bonfils, X., Bouchy, F., Debondt, K., Deleuil, M., Delfosse, X., Desort, M., Díaz, R. F., Eggenberger, A., Ehrenreich, D., Forveille, T., Hébrard, G., Loeillet, B., Lovis, C., Montagnier, G., Moutou, C., Pepe, F., Perrier, C., Pont, F., Queloz, D., Santerne, A., Santos, N. C., Ségransan, D., da Silva, R., Sivan, J. P., Udry, S., and Vidal-Madjar, A., “Extrasolar planets and brown dwarfs around AF-type stars. X. The SOPHIE sample: combining the SOPHIE and HARPS surveys to compute the close giant planet mass-period distribution around AF-type stars,” **621**, A87 (Jan. 2019).

[5] Lloyd, J. P., “Retired” Planet Hosts: Not So Massive, Maybe Just Portly After Lunch,” **739**, L49 (Oct. 2011).

[6] Ghezzi, L., Montet, B. T., and Johnson, J. A., “Retired A Stars Revisited: An Updated Giant Planet Occurrence Rate as a Function of Stellar Metallicity and Mass,” **860**, 109 (June 2018).

[7] Gardner, T., Monnier, J. D., Fekel, F. C., Schaefer, G., Johnson, K. J. C., Le Bouquin, J.-B., Kraus, S., Anugu, N., Setterholm, B. R., Labdon, A., Davies, C. L., Lanthermann, C., Ennis, J., Ireland, M., Kratter, K. M., Ten Brummelaar, T., Sturmann, J., Sturmann, L., Farrington, C., Gies, D. R., Klement, R., and Adams, F. C., “ARMADA. I. Triple Companions Detected in B-type Binaries  $\alpha$  Del and  $\nu$  Gem,” **161**, 40 (Jan. 2021).

[8] Anugu, N., Le Bouquin, J.-B., Monnier, J. D., Kraus, S., Setterholm, B. R., Labdon, A., Davies, C. L., Lanthermann, C., Gardner, T., Ennis, J., Johnson, K. J. C., Ten Brummelaar, T., Schaefer, G., and Sturmann, J., “MIRC-X: A Highly Sensitive Six-telescope Interferometric Imager at the CHARA Array,” **160**, 158 (Oct. 2020).

[9] ten Brummelaar, T. A., McAlister, H. A., Ridgway, S. T., Bagnuolo, Jr., W. G., Turner, N. H., Sturmann, L., Sturmann, J., Berger, D. H., Ogden, C. E., Cadman, R., Hartkopf, W. I., Hopper, C. H., and Shure, M. A., “First Results from the CHARA Array. II. A Description of the Instrument,” **628**, 453–465 (July 2005).

[10] Gravity Collaboration, Abuter, R., Accardo, M., Amorim, A., Anugu, N., Ávila, G., Azouaoui, N., Benisty, M., Berger, J. P., Blind, N., Bonnet, H., Bourget, P., Brandner, W., Brast, R., Buron, A., Burtscher, L., Cassaing, F., Chapron, F., Choquet, É., Clénet, Y., Collin, C., Coudé Du Foresto, V., de Wit, W., de Zeeuw, P. T., Deen, C., Delplancke-Ströbele, F., Dembet, R., Derie, F., Dexter, J., Duvert, G., Ebert, M., Eckart, A., Eisenhauer, F., Esselborn, M., Fédou, P., Finger, G., Garcia, P., Garcia Dabo, C. E., Garcia Lopez, R., Gendron, E., Genzel, R., Gillessen, S., Gonte, F., Gordo, P., Gould, M., Grözinger, U., Guieu, S., Haguenauer, P., Hans, O., Haubois, X., Haug, M., Haussmann, F., Henning, T., Hippler, S., Horrobin, M., Huber, A., Hubert, Z., Hubin, N., Hummel, C. A., Jakob, G., Janssen, A., Jochum, L., Jocou, L., Kaufer, A., Kellner, S., Kendrew, S., Kern, L., Kervella, P., Kiekebusch, M., Klein, R., Kok, Y., Kolb, J., Kulas, M., Lacour, S., Lapeyrère, V., Lazareff, B., Le Bouquin, J. B., Lèna, P., Lenzen, R., Lévéque, S., Lippa, M., Magnard, Y., Mehrgan, L., Mellein, M., Mérand, A., Moreno-Ventas, J., Moulin, T., Müller, E., Müller, F., Neumann, U., Oberti, S., Ott, T., Pallanca, L., Panduro, J., Pasquini, L., Paumard, T., Percheron, I., Perraut, K., Perrin, G., Pflüger, A., Pfuhl, O., Phan Duc, T., Plewa, P. M., Popovic, D., Rabien, S., Ramírez, A., Ramos, J., Rau, C., Riquelme, M., Rohloff, R. R., Rousset, G., Sanchez-Bermudez, J., Scheithauer, S., Schöller, M., Schuhler, N., Spyromilio, J., Straubmeier, C., Sturm, E., Suarez, M., Tristram, K. R. W., Ventura, N., Vincent, F., Waisberg, I., Wank, I., Weber, J., Wiegrecht, E., Wiest, M., Wierzorek, E., Wittkowski, M., Woillez, J., Wolff, B., Yazici, S., Ziegler, D., and Zins, G., “First light for GRAVITY: Phase referencing optical interferometry for the Very Large Telescope Interferometer,” **602**, A94 (June 2017).

[11] Rauscher, E. and Menou, K., “Three-dimensional Atmospheric Circulation Models of HD 189733b and HD 209458b with Consistent Magnetic Drag and Ohmic Dissipation,” **764**, 103 (Feb. 2013).

[12] Kataria, T., Showman, A. P., Fortney, J. J., Marley, M. S., and Freedman, R. S., “The Atmospheric Circulation of the Super Earth GJ 1214b: Dependence on Composition and Metallicity,” **785**, 92 (Apr. 2014).

[13] Diamond-Lowe, H., Stevenson, K. B., Bean, J. L., Line, M. R., and Fortney, J. J., “New Analysis Indicates No Thermal Inversion in the Atmosphere of HD 209458b,” **796**, 66 (Nov. 2014).

[14] Evans, T. M., Sing, D. K., Kataria, T., Goyal, J., Nikolov, N., Wakeford, H. R., Deming, D., Marley, M. S., Amundsen, D. S., Ballester, G. E., Barstow, J. K., Ben-Jaffel, L., Bourrier, V., Buchhave, L. A., Cohen, O., Ehrenreich, D., García Muñoz, A., Henry, G. W., Knutson, H., Lavvas, P., Lecavelier Des Etangs, A., Lewis, N. K., López-Morales, M., Mandell, A. M., Sanz-Forcada, J., Tremblin, P., and Lupu, R., “An ultrahot gas-giant exoplanet with a stratosphere,” **548**, 58–61 (Aug. 2017).

[15] Nowak, M., Lacour, S., Lagrange, A. M., Rubini, P., Wang, J., Stolker, T., Abuter, R., Amorim, A., Asensio-Torres, R., Bauböck, M., Benisty, M., Berger, J. P., Beust, H., Blunt, S., Boccaletti, A., Bonnefoy, M., Bonnet, H., Brandner, W., Cantalloube, F., Charnay, B., Choquet, E., Christiaens, V., Clénet, Y., Coudé Du Foresto, V., Cridland, A., de Zeeuw, P. T., Dembet, R., Dexter, J., Drescher, A., Duvert, G., Eckart, A., Eisenhauer, F., Gao, F., Garcia, P., Garcia Lopez, R., Gardner, T., Gendron, E., Genzel, R., Gillessen, S., Girard, J., Grandjean, A., Haubois, X., Heiβel, G., Henning, T., Hinkley, S., Hippler, S., Horrobin, M., Houllé, M., Hubert, Z., Jiménez-Rosales, A., Jocou, L., Kammerer, J., Kervella, P., Keppler, M., Kreidberg, L., Kulikauskas, M., Lapeyrère, V., Le Bouquin, J. B., Léna, P., Mérand, A., Maire, A. L., Mollière, P., Monnier, J. D., Mouillet, D., Müller, A., Nasedkin, E., Ott, T., Otten, G., Paumard, T., Paladini, C., Perraut, K., Perrin, G., Pueyo, L., Pfuhl, O., Rameau, J., Rodet, L., Rodríguez-Coira, G., Rousset, G., Scheithauer, S., Shangguan, J., Stadler, J., Straub, O., Straubmeier, C., Sturm, E., Tacconi, L. J., van Dishoeck, E. F., Vigan, A., Vincent, F., von Fellenberg, S. D., Ward-Duong, K., Widmann, F., Weprecht, E., Wiesorrek, E., Woillez, J., and Gravity Collaboration, “Direct confirmation of the radial-velocity planet  $\beta$  Pictoris c,” **642**, L2 (Oct. 2020).

[16] Zhao, M., Monnier, J. D., Che, X., Pedretti, E., Thureau, N., Schaefer, G., ten Brummelaar, T., Mérand, A., Ridgway, S. T., McAlister, H., Turner, N., Sturmann, J., Sturmann, L., Goldfinger, P. J., and Farrington, C., “Toward Direct Detection of Hot Jupiters with Precision Closure Phase: Calibration Studies and First Results from the CHARA Array,” **123**, 964 (Aug. 2011).

[17] Anugu, N., Monnier, J. D., Le Bouquin, J.-B., and Kraus, S., “CHARA MIRC-X and MYSTIC cophasing observations to enable efficient spectro-interferometry and over-resolved object imaging,” in [*Optical and Infrared Interferometry and Imaging VIII*], Merand, A., Sallum, S., and Sanchez-Bermudez, J., eds., *Society of Photo-Optical Instrumentation Engineers (SPIE) Conference Series* **12183**, 12183–18 (July 2022).

[18] Perryman, M., Hartman, J., Bakos, G. Á., and Lindegren, L., “Astrometric Exoplanet Detection with Gaia,” **797**, 14 (Dec. 2014).

[19] Gardner, T., Monnier, J. D., Fekel, F. C., Williamson, M., Duncan, D. K., White, T. R., Ireland, M., Adams, F. C., Barman, T., Baron, F., ten Brummelaar, T., Che, X., Huber, D., Kraus, S., Roettenbacher, R. M., Schaefer, G., Sturmann, J., Sturmann, L., Swihart, S. J., and Zhao, M., “Precision Orbit of  $\delta$  Delphini and Prospects for Astrometric Detection of Exoplanets,” **855**, 1 (Mar 2018).

[20] Kraus, A. L., Ireland, M. J., Huber, D., Mann, A. W., and Dupuy, T. J., “The Impact of Stellar Multiplicity on Planetary Systems. I. The Ruinous Influence of Close Binary Companions,” **152**, 8 (July 2016).

[21] Sanchez-Bermudez, J., Alberdi, A., Barbá, R., Bestenlehner, J. M., Cantalloube, F., Brandner, W., Henning, T., Hummel, C. A., Maíz Apellániz, J., Pott, J. U., Schödel, R., and van Boekel, R., “GRAVITY Spectro-interferometric Study of the Massive Multiple Stellar System HD 93206 A,” **845**, 57 (Aug. 2017).

[22] Monnier, J. D., Che, X., Zhao, M., Ekström, S., Maestro, V., Aufdenberg, J., Baron, F., Georgy, C., Kraus, S., McAlister, H., Pedretti, E., Ridgway, S., Sturmann, J., Sturmann, L., ten Brummelaar, T., Thureau, N., Turner, N., and Tuthill, P. G., “Resolving Vega and the Inclination Controversy with CHARA/MIRC,” **761**, L3 (Dec. 2012).

[23] Motalebi, F., Udry, S., Gillon, M., Lovis, C., Ségransan, D., Buchhave, L. A., Demory, B. O., Malavolta, L., Dressing, C. D., Sasselov, D., Rice, K., Charbonneau, D., Collier Cameron, A., Latham, D., Molinari, E., Pepe, F., Affer, L., Bonomo, A. S., Cosentino, R., Dumusque, X., Figueira, P., Fiorenzano, A. F. M., Gettel, S., Harutyunyan, A., Haywood, R. D., Johnson, J., Lopez, E., Lopez-Morales, M., Mayor, M., Micela, G., Mortier, A., Nascimbeni, V., Philips, D., Piotto, G., Pollacco, D., Queloz, D., Sozzetti, A., Vanderburg, A., and Watson, C. A., “The HARPS-N Rocky Planet Search. I. HD 219134 b: A transiting rocky planet in a multi-planet system at 6.5 pc from the Sun,” **584**, A72 (Dec. 2015).

[24] Sato, B., Hirano, T., Omiya, M., Harakawa, H., Kobayashi, A., Hasegawa, R., Takarada, T., Kawauchi, K., and Masuda, K., “Precise Radial Velocity Measurements for Kepler Giants Hosting Planetary Candidates: Kepler-91 and KOI-1894,” **802**, 57 (Mar. 2015).

- [25] Feng, F., Tuomi, M., Jones, H. R. A., Butler, R. P., and Vogt, S., “A Goldilocks principle for modelling radial velocity noise,” **461**, 2440–2452 (Sept. 2016).
- [26] Malsky, I., Rauscher, E., Kempton, E. M. R., Roman, M., Long, D., and Harada, C. K., “Modeling the High-resolution Emission Spectra of Clear and Cloudy Nontransiting Hot Jupiters,” **923**, 62 (Dec. 2021).
- [27] Rauscher, E. and Menou, K., “A General Circulation Model for Gaseous Exoplanets with Double-gray Radiative Transfer,” **750**, 96 (May 2012).
- [28] Roman, M. and Rauscher, E., “Modeling the Effects of Inhomogeneous Aerosols on the Hot Jupiter Kepler-7b’s Atmospheric Circulation,” **850**, 17 (Nov. 2017).
- [29] Piskorz, D., Benneke, B., Crockett, N. R., Lockwood, A. C., Blake, G. A., Barman, T. S., Bender, C. F., Carr, J. S., and Johnson, J. A., “Detection of Water Vapor in the Thermal Spectrum of the Non-transiting Hot Jupiter Upsilon Andromedae b,” **154**, 78 (Aug. 2017).
- [30] Monnier, J. D., Le Bouquin, J.-B., Anugu, N., Kraus, S., Setterholm, B. R., Ennis, J., Lanthermann, C., Jocou, L., and ten Brummelaar, T., “MYSTIC: Michigan Young STar Imager at CHARA,” in [*Optical and Infrared Interferometry and Imaging VI*], Creech-Eakman, M. J., Tuthill, P. G., and Mérand, A., eds., *Society of Photo-Optical Instrumentation Engineers (SPIE) Conference Series* **10701**, 1070122 (July 2018).
- [31] Setterholm, B. R., Monnier, J. D., Le Bouquin, J.-B., and Anugu, N., “MYSTIC: a high angular resolution K-band imager at CHARA,” in [*Optical and Infrared Interferometry and Imaging VIII*], Merand, A., Sallum, S., and Sanchez-Bermudez, J., eds., *Society of Photo-Optical Instrumentation Engineers (SPIE) Conference Series* **12183**, 12183–10 (July 2022).
- [32] Gaia Collaboration, Brown, A. G. A., Vallenari, A., Prusti, T., de Bruijne, J. H. J., Babusiaux, C., Biermann, M., Cleevey, O. L., Evans, D. W., Eyer, L., Hutton, A., Jansen, F., Jordi, C., Klioner, S. A., Lammers, U., Lindegren, L., Luri, X., Mignard, F., Panem, C., Pourbaix, D., Randich, S., Sartoretti, P., Soubiran, C., Walton, N. A., Arenou, F., Bailer-Jones, C. A. L., Bastian, U., Cropper, M., Drimmel, R., Katz, D., Lattanzi, M. G., van Leeuwen, F., Bakker, J., Cacciari, C., Castañeda, J., De Angeli, F., Ducourant, C., Fabricius, C., Fouesneau, M., Frémat, Y., Guerra, R., Guerrier, A., Guiraud, J., Jean-Antoine Piccolo, A., Masana, E., Messineo, R., Mowlavi, N., Nicolas, C., Nienartowicz, K., Pailler, F., Panuzzo, P., Riclet, F., Roux, W., Seabroke, G. M., Sordo, R., Tanga, P., Thévenin, F., Gracia-Abril, G., Portell, J., Teyssier, D., Altmann, M., Andrae, R., Bellas-Velidis, I., Benson, K., Berthier, J., Blomme, R., Brugaletta, E., Burgess, P. W., Busso, G., Carry, B., Cellino, A., Cheek, N., Clementini, G., Damerdji, Y., Davidson, M., Delchambre, L., Dell’Oro, A., Fernández-Hernández, J., Galluccio, L., García-Lario, P., Garcia-Reinaldos, M., González-Núñez, J., Gosset, E., Haigron, R., Halbwachs, J. L., Hambly, N. C., Harrison, D. L., Hatzidimitriou, D., Heiter, U., Hernández, J., Hestroffer, D., Hodgkin, S. T., Holl, B., Janßen, K., Jevardat de Fombelle, G., Jordan, S., Krone-Martins, A., Lanzafame, A. C., Löffler, W., Lorca, A., Manteiga, M., Marchal, O., Marrese, P. M., Moitinho, A., Mora, A., Muinonen, K., Osborne, P., Pancino, E., Pauwels, T., Petit, J. M., Recio-Blanco, A., Richards, P. J., Riello, M., Rimoldini, L., Robin, A. C., Roegiers, T., Rybizki, J., Sarro, L. M., Siopis, C., Smith, M., Sozzetti, A., Ulla, A., Utrilla, E., van Leeuwen, M., van Reeven, W., Abbas, U., Abreu Aramburu, A., Accart, S., Aerts, C., Aguado, J. J., Ajaj, M., Altavilla, G., Álvarez, M. A., Álvarez Cid-Fuentes, J., Alves, J., Anderson, R. I., Anglada Varela, E., Antoja, T., Audard, M., Baines, D., Baker, S. G., Balaguer-Núñez, L., Balbinot, E., Balog, Z., Barache, C., Barbato, D., Barros, M., Barstow, M. A., Bartolomé, S., Bassilana, J. L., Bauchet, N., Baudesson-Stella, A., Becciani, U., Bellazzini, M., Bernet, M., Bertone, S., Bianchi, L., Blanco-Cuaresma, S., Boch, T., Bombrun, A., Bossini, D., Bouquillon, S., Bragaglia, A., Bramante, L., Breedt, E., Bressan, A., Brouillet, N., Bucciarelli, B., Burlacu, A., Busonero, D., Butkevich, A. G., Buzzi, R., Caffau, E., Cancelliere, R., Cánovas, H., Cantat-Gaudin, T., Carballo, R., Carlucci, T., Carnerero, M. I., Carrasco, J. M., Casamiquela, L., Castellani, M., Castro-Ginard, A., Castro Sampol, P., Chaoul, L., Charlot, P., Chemin, L., Chiavassa, A., Cioni, M. R. L., Comoretto, G., Cooper, W. J., Cornez, T., Cowell, S., Crifo, F., Crosta, M., Crowley, C., Dafonte, C., Dapergolas, A., David, M., David, P., de Laverny, P., De Luise, F., De March, R., De Ridder, J., de Souza, R., de Teodoro, P., de Torres, A., del Peloso, E. F., del Pozo, E., Delbo, M., Delgado, A., Delgado, H. E., Delisle, J. B., Di Matteo, P., Diakite, S., Diener, C., Distefano, E., Dolding, C., Eappachen, D., Edvardsson, B., Enke, H., Esquej, P., Fabre, C., Fabrizio, M., Faigler, S., Fedorets, G., Fernique, P., Fienga, A., Figueras, F., Fouron, C., Frakoudi, F., Fraile, E., Franke, F., Gai, M., Garabato, D., Garcia-Gutierrez, A., García-Torres, M., Garofalo, A., Gavras, P., Gerlach, E., Geyer, R., Giacobbe, P., Gilmore, G., Girona, S., Giuffrida, G.,

Gomel, R., Gomez, A., Gonzalez-Santamaria, I., González-Vidal, J. J., Granvik, M., Gutiérrez-Sánchez, R., Guy, L. P., Hauser, M., Haywood, M., Helmi, A., Hidalgo, S. L., Hilger, T., Hładczuk, N., Hobbs, D., Holland, G., Huckle, H. E., Jasniewicz, G., Jonker, P. G., Juaristi Campillo, J., Julbe, F., Karbevska, L., Kervella, P., Khanna, S., Kochoska, A., Kontizas, M., Kordopatis, G., Korn, A. J., Kostrzewska-Rutkowska, Z., Kruszyńska, K., Lambert, S., Lanza, A. F., Lasne, Y., Le Campion, J. F., Le Fustec, Y., Lebreton, Y., Lebzelter, T., Leccia, S., Leclerc, N., Lecoeur-Taibi, I., Liao, S., Licata, E., Lindstrøm, E. P., Lister, T. A., Livanou, E., Lobel, A., Madrero Pardo, P., Managau, S., Mann, R. G., Marchant, J. M., Marconi, M., Marcos Santos, M. M. S., Marinoni, S., Marocco, F., Marshall, D. J., Martin Polo, L., Martín-Fleitas, J. M., Masip, A., Massari, D., Mastrobuono-Battisti, A., Mazeh, T., McMillan, P. J., Messina, S., Michalik, D., Millar, N. R., Mints, A., Molina, D., Molinaro, R., Molnár, L., Montegriffo, P., Mor, R., Morbidelli, R., Morel, T., Morris, D., Mulone, A. F., Munoz, D., Muraveva, T., Murphy, C. P., Musella, I., Noval, L., Ordénovic, C., Orrù, G., Osinde, J., Pagani, C., Pagano, I., Palaversa, L., Palicio, P. A., Panahi, A., Pawlak, M., Peñalosa Esteller, X., Penttilä, A., Piersimoni, A. M., Pineau, F. X., Plachy, E., Plum, G., Poggio, E., Poretti, E., Poujoulet, E., Prša, A., Pulone, L., Racero, E., Ragaini, S., Rainer, M., Raiteri, C. M., Rambaux, N., Ramos, P., Ramos-Lerate, M., Re Fiorentin, P., Regibo, S., Reylé, C., Ripepi, V., Riva, A., Rixon, G., Robichon, N., Robin, C., Roelens, M., Rohrbasser, L., Romero-Gómez, M., Rowell, N., Royer, F., Rybicki, K. A., Sadowski, G., Sagristà Sellés, A., Sahlmann, J., Salgado, J., Salguero, E., Samaras, N., Sanchez Gimenez, V., Sanna, N., Santoveña, R., Sarasso, M., Schultheis, M., Sciacca, E., Segol, M., Segovia, J. C., Ségransan, D., Semeux, D., Shahaf, S., Siddiqui, H. I., Siebert, A., Siltala, L., Slezak, E., Smart, R. L., Solano, E., Solitro, F., Souami, D., Souchay, J., Spagna, A., Spoto, F., Steele, I. A., Steidelmüller, H., Stephenson, C. A., Süveges, M., Szabados, L., Szegedi-Elek, E., Taris, F., Tauran, G., Taylor, M. B., Teixeira, R., Thuillot, W., Tonello, N., Torra, F., Torra, J., Turon, C., Unger, N., Vaillant, M., van Dillen, E., Vanel, O., Vecchiato, A., Viala, Y., Vicente, D., Voutsinas, S., Weiler, M., Wevers, T., Wyrzykowski, L., Yoldas, A., Yvard, P., Zhao, H., Zorec, J., Zucker, S., Zurbach, C., and Zwitter, T., “Gaia Early Data Release 3. Summary of the contents and survey properties,” **649**, A1 (May 2021).

[33] Buzard, C., Piskorz, D., Lockwood, A. C., Blake, G., Barman, T. S., Benneke, B., Bender, C. F., and Carr, J. S., “Reinvestigation of the Multiepoch Direct Detections of HD 88133 b and Upsilon Andromedae b,” **162**, 269 (Dec. 2021).

[34] Newville, M., Stensitzki, T., Allen, D. B., Rawlik, M., Ingargiola, A., and Nelson, A., “Lmfit: Non-Linear Least-Square Minimization and Curve-Fitting for Python,” (Jun 2016).

[35] Sahlmann, J., Martín-Fleitas, J., Mora, A., Abreu, A., Crowley, C. M., and Joliet, E., “Enabling science with Gaia observations of naked-eye stars,” in [*Space Telescopes and Instrumentation 2016: Optical, Infrared, and Millimeter Wave*], **9904**, 99042E (July 2016).

[36] Ireland, M. J. and Woillez, J., “Astrometric Interferometry,” *arXiv e-prints* , arXiv:1812.02926 (Dec. 2018).